LASER-BOOSTED LIGHTCRAFT TECHNOLOGY DEMONSTRATOR*

J. C. Richard,† C. Morales,‡ W. L. Smith,§ and L. N. Myrabo¶

Rensselaer Polytechnic Institute
Troy, NY 12181

Abstract

The detailed description and performance analysis of a 1.4 meter diameter Lightcraft Technology Demonstrator (LTD) is presented. The novel launch system employs a 100 MW-class ground-based laser to transmit power directly to an advanced combined-cycle engine that propels the 120 kg LTD to orbit — with a mass ratio of two. The single-stage-to-orbit (SSTO) LTD machine then becomes an autonomous sensor satellite that can deliver precise, high quality information typical of today's large orbital platforms.

The dominant motivation behind this study is to provide an example of how laser propulsion and its low launch costs can induce a comparable order-of-magnitude reduction in sensor satellite packaging costs. The issue is simply one of production technology for future, survivable SSTO aerospace vehicles that intimately share both laser propulsion engine and satellite functional hardware.

Introduction

In order for laser propulsion to enable a significant reduction in the cost of certain critical space systems, both launch and payload costs must be reduced by (at least) an order of magnitude. Canavan[1] was first to bring this fact to light, noting that a reduction in either category alone would have much less economic impact. This conclusion emerged from recent in-depth examinations of the economics for laser propulsion deployment of sensors, interceptors and decoys.[1,2] Furthermore, Canavan affirms that the minimum effective system must be able to launch 60–100 kg payloads. After evaluating cost projections, he concludes that a system designed for payloads smaller than this could increase costs significantly, reducing laser propulsion's margin with respect to both the threat and conventional chemical rocket alternatives.[1]

Apparently, the true costs of building and launching today's large satellite platforms are not widely known, as discussed in a recent *Aerospace America* article.[3] For example, sensor hardware can cost upwards of $200,000/kg and to put that sensor into geostationary orbit (GEO) typically requires $10,000/kg of payload. Flying the Shuttle Orbiter to a 250 km low Earth orbit may cost $3000/lb, but the actual price is really almost twice that amount because the shuttle itself is *not* amortized against the payload.[4] The projected launch cost goal for the Advanced Launch System (ALS) is roughly $300/lb to LEO. Hence, for laser propulsion to play a significant role in boosting future critical space systems, launch costs must fall to $100/kg or below.

Canavan has raised the fascinating issue of whether and how laser propulsion and its low launch costs could induce a substantial reduction in satellite package costs.[1] In the opinion of the authors, such reductions could be facilitated by an exceptionally close integration of the laser propulsive engine and satellite functional hardware. Pushed to the extreme, almost every vehicle component could be designed to serve multiple functions, in both transatmospheric and orbital flight modes.

Clearly, the ultimate configuration of any laser-boosted machine will be strongly driven, if not entirely dominated, by the mission it must perform; be it interceptor, decoy or sensor. A near infinite number of successful configurations could be alleged to exist, but it is most instructive to select a *specific mission*, and then to explore a single configuration from the initial design concept, through the preliminary engineering design process.

The advanced aerospace vehicle considered here is exemplary of a class of sensor machines that can be derived largely from an intimate integration of propulsion and sensor systems. The proposed design exploits the inherent advantages of advanced beamed-energy sources (i.e., high power lasers) and innovative combined-cycle (airbreathing/rocket) engines to accomplish this goal. The authors believe that this unique approach could ultimately enable a reduction in launch and sensor package costs by one or two orders of magnitude below present levels. However, as pointed out by Canavan,[1] the numbers of these sensor satellites may not be great enough to justify the expense of the entire laser launch facility for this application alone. Nevertheless, the launch facility is likely to be amortized over a great number of users and dissimilar mission applications anyway.

*This research was sponsored by Lawrence Livermore National Laboratory, Subcontract No. 2073803, under the Laser Propulsion Program of the SDIO.

†Graduate student, Aeronautical Engineering.
‡Undergraduate student, Mechanical Engineering.
§Graduate student, Mechanical Engineering.
¶Assistant Professor, Mechanical Engineering.

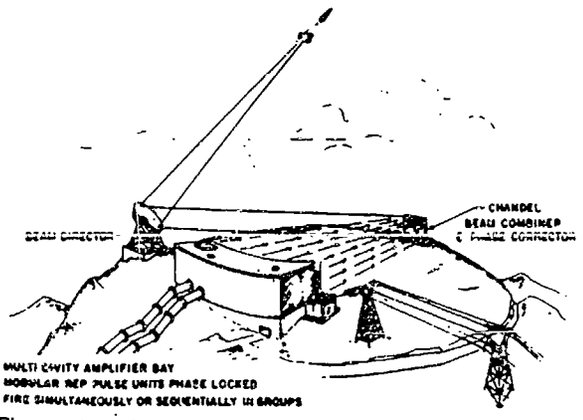

Figure 1: Ground Based CO_2 Laser System [After Kantrowitz]

Ground-based Laser Launch Facility

Portrayed in Fig. 1 is a 100 MW-class ground based laser (GBL) that could be built with existing closed-cycle CO_2 laser technology using E-beam pumping. A powerful CO_2 electric laser could be fabricated in the next 4–5 years by assembling numerous (e.g., 100) smaller units (e.g., 1–3 MW each) into a large array. Redundant units would be built into the system so that inoperative units could be dropped out, with no loss in system utility. As shown in Fig. 1, a Chandel-type beam combiner could then be invoked to link all the output beams together.

All the units could be fired *simultaneously* to give the lowest pulse repetition frequency (PRF) of perhaps several hundred Hertz at the highest pulse energy (E_p); at the other extreme, each unit could be triggered *sequentially* to yield the lowest E_p's and PRF's up to 10 kHz. Using E-beam pumping, laser pulse durations (t_p) can be limited to the range 0.1 to 1.0 μsec which smaller, near-term pulsed laser propulsion engines will require.

Configured in this manner, the GBL facility can be programmed to deliver a complicated pulse train sequence of PRF's, E_p's and t_p's with the utmost of ease. This pulse train can be calculated to exactly match what a laser propulsion engine will need along a given launch trajectory — i.e., normally a direct function of flight Mach number and altitude. The goal is to produce an efficient thruster without introducing too much flight hardware, which has added so much to the cost of chemical rockets, as Kantrowitz has observed.[4]

The essential point of this advanced launch scheme is to place as much of the system complexity as possible *on the ground* (no weight penalty here!), where it can be serviced easily. With this approach, laser-powered thrusters can be reduced to their simplest, and most reliable configuration.

The "straw man" GBL facility suggested here is set at the 250 MW level which is adequate to launch a 120 kg (dry mass), 1.4 meter diameter Lightcraft Technology Demonstrator (LTD) to low Earth orbit. The range of laser pulse energies required by its combined-cycle (airbreathing/rocket) engine is 40 KJ $< E_p <$ 70 KJ; PRF varies from 200 Hz to 10 KHz, and t_p varies from 0.3 to 0.4 μsec — depending on the exact trajectory (i.e., Mach number vs. altitude) flown to orbit. With these parameters, the peak flux across the 1.0 m diameter LTD primary optic will fall in the range of 13.0 to 30.0 MW/cm^2.

This large GBL facility is a near term reality that exploits fifteen year old CO_2 laser technology. Kantrowitz[5] notes that the important costs for the CO_2 GBL installation, are for capital and operating expenses (which might add another 20% of the capital cost per year). Refer to Ref. [5] for an in-depth accounting of the economics for a GBL launch facility. However, for the long term, the Free Electron Laser (FEL) is the favored future system due to its promise of high electric-to-laser conversion efficiency and reliability.

Aerospace Vehicle Concept

Kantrowitz[5] has noted that to make laser propulsion a serious contender for space transportation to LEO, we will need to develop propellants that can achieve high thruster efficiency at low incident laser flux levels. It is also apparent that atmospheric transmission problems must be considered, especially in the immediate vicinity of the vehicle where the beam must propagate unhampered through the thruster's rapidly expanding, and potentially absorbing, exhaust.

Adaptive transmitter optics can be invoked to successfully bring the power beam up through the atmosphere. The 10 m diameter beam-director mirror suggested by Kantrowitz[5] would allow a 10 μm beam to be focused on a one meter diameter vehicle base, out to a range of about 800 km. This performance is, of course, close to the diffraction limit.

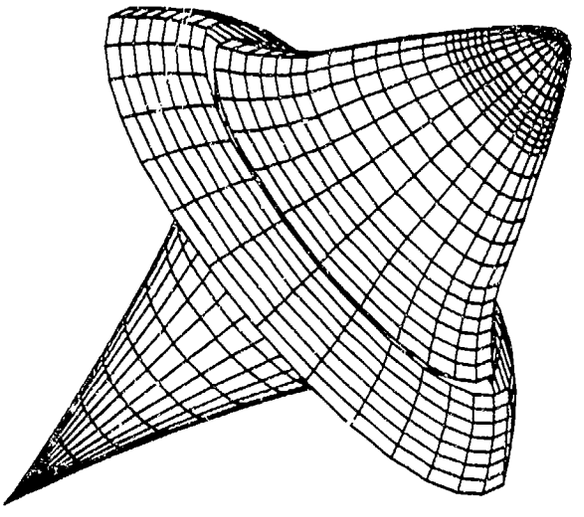

Figure 2: Lightcraft Technology Demonstrator (1.4 meter diameter)

It is the opinion of the authors that focusing mirrors mounted on the laser propelled vehicle are the most expedient way to permit both low flux levels in the atmospheric transmission link and elevated flux levels within the thruster (which are required for high propulsive efficiency). The reference "point design" for the Lightcraft Technology Demonstrator is configured around a 1.0 meter diameter parabolic mirror, as shown in Fig. 2. This primary receptive optical surface comprises the entire vehicle afterbody, which also serves as a plug nozzle for the laser-heated thruster.

In a related laser propulsion design effort at RPI last Fall (1987), The Apollo Lightcraft Project,[6,7] it was discovered that such a primary optic (PO) could also serve as a *telescopic lens* when not being used in the propulsive mode. Likewise, the LTD's 1.0 meter mirror could be "plugged-in" to the sensor function once it is in orbit. For example, it is known that optics in the 0.5 to 1.0 meter diameter range could well serve the purposes of midcourse tracking satellites positioned at altitudes of 1000 to 2000 km. Smaller PO's (e.g., 0.33 m) would be more suitable for reconnaissance satellites located in 200 to 500 km orbits.

This leaves the remaining problems of propagating the beam through the propulsive engine's exhaust, and of keeping the receptive PO mirror from melting down. As will soon become apparent, the two problems are found to be clearly interrelated. Most of today's high power CO_2 laser optics used under laboratory conditions are found to be water-cooled copper mirrors, sometimes silver coated, with a reflectivity of 99% (at best). These mirrors are heavy and the technology is not easily adaptable to the kind of lightweight design required for flight applications.

On the other hand, cryogenic-cooled, diamond-turned aluminum mirrors look especially promising. The 1.0 m diameter LTD mirror could easily be cut on Lawrence Livermore National Lab's LODTM, a state-of-the-art Large Optics Diamond Turning Machine. This lightweight, large optic technology is being developed for SDI applications, and reflectivities of uncoated surfaces have been pushed to 98% — which is close to the theoretical limit for aluminum. Various silver coating processes have been applied to improve the reflectivity of other high temperature faceplates such as titanium, molybdenum, beryllium/copper alloys (or perhaps stainless steel), but they cannot be expected to survive the abusive thermomechanical environment within a pulsed laser propulsion engine.

Hence, a cryogenic or water-cooled 3000–5000 series aluminum mirror appears to be the best candidate. A transparent, hard, protective coating such as aluminum oxide, silicon oxide, or vapor-deposited diamond must be applied over the bare aluminum to serve as an oxygen barrier. Water is an excellent coolant, its heat transfer characteristics are well known, and sacrificial coolant could be vented as high pressure steam to cool the mirror during engine operation.

However, CO_2 laser radiation is heavily absorbed by water vapor, so a dense steam wake behind the craft may prevent proper transmission and focusing of the beam into the LTD's engine. An alternative would be to utilize isotropic CO_2 in the GBL to shift the spectrum away from H_2O vapor absorption lines; for the future free electron lasers, wavelength could be independently chosen to deliberately avoid the H_2O vapor issue. Another problem with the use of H_2O as a coolant is that condensed water droplets have been known to trigger localized damage on coated high power optics irradiated with pulsed beams.

In the rocket mode, the coolant will also serve as the reaction propellant, and regeneratively cool the rocket nozzle (mirror) along with other hot components. Clearly, one desires a propellant with the lowest molecular weight, such as H_2. Liquid hydrogen, unfortunately, has such a high specific volume that only 14 kg of LH_2 could be stored in the LTD's 70 cm diameter fuel tank. This is more than a factor of 10 too small.

For a number of reasons, then, LN_2 appears to be an ideal propellant for use in the LTD, and its specific gravity is 80.8% that of water. Heated to high temperature and pressure, nitrogen should produce specific impulses (I_{sp}) in the range of 725 to 1025 seconds — depending on whether the ejected gas is dissociated or not. This should produce thrust coupling coefficients (CC) of roughly 100 N/MW for a 40% efficient conversion process. Note that CC, η_{th} and I_{sp} are related by:

$$\mathrm{CC} = \frac{2\eta_{th}}{gI_{sp}} \times 10^6, \quad (\mathrm{N/MW}) \tag{1}$$

where g is acceleration due to gravity (9.8 m/s^2), I_{sp} is in seconds, η_{th} is the thruster efficiency and CC is in N/MW.

LN_2 is also favored because it is an inert and exceptionally clean propellant (especially important for high power optics), whose physical properties closely match those of air, which is 78% N_2 by volume. Hence, one would also expect that a combined-cycle pulsed laser propulsion engine would have little difficulty in shifting modes from *airbreathing* to rocket operation.

With regard to pulsed laser damage thresholds and active cooling limits of aluminum mirrors, the following comments can be made. The current time-average maximum absorbed flux limit for water-cooled copper mirrors with good optical figures is 200 W/cm^2. The single pulse safe operating limits (S.O.L.) for high power laser mirrors (see Ref. [8]) are:

$$\mathrm{S.O.L.} = \frac{F_\perp \sin\phi}{\sqrt{t_p}} \leq 10^4 \frac{\mathrm{J}}{\mathrm{cm^2 sec^{\frac{1}{2}}}} \tag{2}$$

where $F_\perp$ is the perpendicular incident fluence, t_p is the laser pulse duration, and ϕ is the inclination of the surface to the incident laser beam. This operational limit assumes a factor of 10× safety margin below the actual catastrophic damage limit of 10^5 J/(cm^{2}sec$^{\frac{1}{2}}$).

For the LTD parabolic mirror shown in Fig. 2, note that the surface is inclined at the greatest angle along the beam centerline, where the laser flux is highest. For the sake of argument, assume the intensity distribution is gaussian, rather than "top hat" or constant. Most of the laser flux

is received upon the outer annular portion of the mirror surface, which is inclined at an angle of 30° to the axis of symmetry. The conical tip has a half angle of 15°.

Assuming a maximum pulse energy of 70 kJ delivered in 0.3 μsec over the 7854 cm^2 (perpendicular area) LTD optic:

$$30° \Longrightarrow \frac{F_\perp \sin\phi}{\sqrt{t}} = \frac{70{,}000 \times \sin 30°}{7854 \times (0.3 \times 10^{-6})^{\frac{1}{2}}} = 6136 \ \frac{\text{J}}{\text{cm}^2\text{sec}^{\frac{1}{2}}}$$

This is clearly below the 10^4 J/(cm^{2}sec$^{\frac{1}{2}}$) maximum suggested operational limit. Note that the cone tip sees only 4212 J/(cm^{2}sec$^{\frac{1}{2}}$).

The breakdown fluence for aluminum surfaces is known to be roughly 10 J/cm^2. Beyond this limit, a plasma will be ignited on aluminum mirrors. Note that 70 kJ applied uniformly over a perpendicular surface of 7854 cm^2, results in a fluence of 8.9 J/cm^2. However, since most of the LTD's primary optic will be at 30°, this fluence is actually spread over twice the surface area, yielding 4.45 J/cm^2. Hence, plasma ignition on the aluminum does not appear to be a problem, except perhaps for the pointed tip of the parabolic mirror.

The absorbed heat flux (AHF) into the mirror is a function of the reflectivity ρ, local time-average beam intensity P_{ave}, and mirror inclination ϕ.

$$\text{A.H.F} = \left(\frac{P_{ave}}{A_\perp}\right) \sin\phi(1-\rho) \qquad (3)$$

Assuming a time-average laser power of 250 MW with a "top hat" intensity distribution across a 1 m diameter mirror with 98% reflectivity, one finds:

$$30° \Longrightarrow \frac{(250 \times 10^6 \text{ W})(\sin 30°)(0.02)}{7854 \text{ cm}^2} = 318 \ \frac{\text{W}}{\text{cm}^2}$$

For the 15° cone tip, 165 W/cm^2 is absorbed.

Note that the absorbed flux on a 30° surface does exceed the 200 W/cm^2 limit for maintaining a *good* optical figure on the mirror. Although a distortion of several wavelengths is certain to occur, this *crude* figure will still be acceptable for the laser boost — since the focal length is only 60 cm, and the focal ring width is 1 cm. Once the vehicle is in space and the propulsive beam is shut off, the ideal mirror surface would relax to a high quality optical figure needed for an imaging telescope. The goal would be to avoid permanently bending/distorting the lens during the laser boost. Hysteresis effects under these flux conditions must be studied.

Three major issues still need to be investigated: (i) the scattering characteristics of diamond-turned aluminum mirrors at incidence angles of 15° to 45°, (ii) plasma breakdown threshold vs. mirror angle for grazing-incidence mirrors (avoid problem angles of 5° to 10°); and (iii) frost condensation on LN_2 cooled mirror surfaces.

Of the three issues, the last is potentially the most serious. During the laser boost "startup transient," the laser must be turned on first, then the LN_2 coolant valve would be opened. The objective is to prevent any part of the mirror surface from cooling below the dew point. If frost does form on the mirror it cannot perform its focusing function. Also, an ice layer just a few wavelengths thick will trigger full absorption of the incident laser pulse — potentially damaging the optic.

Finally, it should be noted that the harsh vibration and hypersonic aerothermodynamic environment which transatmospheric pulsed laser propulsion will subject onto the satellite sensor systems during the boost to orbit will necessarily make them highly survivable (by design).

Engine/Vehicle Description

The LTD has a dry mass of 120 kg and is filled with 180 kg of LN_2 just prior to launch. A compressed-gas or steam cannon ejects the LTD with an initial velocity of 100–200 m/sec. One half second later, the GBL directs laser power to the vehicle's combined-cycle engine, and an airbreathing propulsion mode accelerates the LTD to Mach 7 and 120 kft. Thereafter, a laser-powered rocket mode (specific impulse $\geq$ 875 sec and CC = 100 N/MW) inserts the LTD into orbit, with 30 kg of liquid nitrogen (ullage) still remaining in the tank. This single-stage-to-orbit vehicle has a mass ratio of 2.0, and the *entire* final mass of 150 kg (i.e., 120 kg dry mass plus 30 kg of LN_2 ullage) becomes the payload.

Once in orbit, the LTD functions as an autonomous sensor satellite that is able to "look out" through its 1 meter diameter primary optic "eye." If this parabolic mirror is polished to optical quality, its resolution limit at 100 μm is 8 cm from an altitude of 180 km, or 17 cm from 360 km (see Table 1). Soon after arriving in orbit, the remaining LN_2 evaporates, thereby cooling down the vehicle, while pressurizing the propellant tank to 4000 psi. This compressed, cold, gaseous N_2 supply is then utilized by a simple 3-axis attitude control system to accomplish fine pointing required for sensor satellite functions throughout its life-

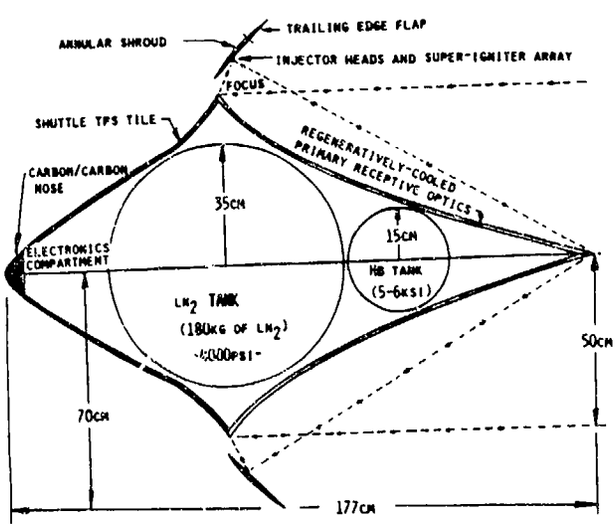

Figure 3: Cutaway View of LTD Aerospace Vehicle

OPTICAL PARAMETER	WAVELENGTH, λ			
	400nm	700nm	10.6μ	1cm
α_0	4.8×10^{-7}	8.54×10^{-7}	12.93×10^{-6}	12.2×10^{-3}
$\alpha(F)^*$	29.28×10^{-9}	512.4×10^{-9}	7.76×10^{-6}	7.32×10^{-3}
α(36,000 Km)	17.28m	30.74	465.48	439.2×10^{3}
α(360 Km)	0.17m	0.30	4.65	4.39×10^{5}
α(180 Km)	0.08m	0.15	2.33	2.19×10^{3}

* FOCAL LENGTH = 60cm (ANGLES IN RADIANS, LENGTHS IN METERS)

Table 1: Resolution Limits for 1.0 m Diameter Mirrors

time. Of the 120 kg dry mass, only 18 kg is reserved for the sophisticated microcircuitry servos, star-tracker, etc. that control both laser-launch and satellite functions. Considering the recent developments in lightsats (Ref. [3]) and microsats, this mass allotment should pose no major problem.

As presently conceived, the LTD vehicle pictured in Fig. 3 could be constructed using state-of-the-art components derived from current liquid chemical rocket engine technology, advanced composite structures, and high power laser optics developed for SDI applications. As mentioned earlier, the regeneratively cooled, 1 m diameter primary optic is to be fabricated from aluminum using diamond-turned mirror technology. Since the reflectivity will be 98% at best, roughly 2% of the incident laser power must be carried away by sacrificial LN_2 coolant during the airbreathing boost mode. In the rocket mode, however, the primary optic will also serve as a plug nozzle: hence, the parallel with liquid chemical rocket technology becomes obvious.

A cutaway view in Fig. 3 shows the internal arrangement of hardware components for the LTD machine. The projected mass breakdown for the vehicle is given in Table 2. Note that the two most massive components are the 70 cm diameter LN_2 tank and the actively cooled 1 m diameter primary optic. The LN_2 tank is a filament wound pressure vessel similar to the ones made by Brunswick Defense in Lincoln, Nebraska. Brunswick makes a 26 in. diameter aluminum-lined spherical Kevlar tank which has a maximum operating pressure of 4,000 psig at 200°F, and a burst pressure of 6,000 psig. The pressure vessel is designed for storage of helium and nitrogen. It has an empty weight of 73.5 lb (33.33 kg).

Primary Receptive Optic

Figure 4 displays the range of primary optic (PO) contours considered for the LTD machine. These contours are generated by rotating a parabola about an off-center axis. Note that the annular shroud airfoil has a circular arc cross-section with a flat bottom, and a chord (C) length of 22.5 cm. Five PO contours are displayed with focal rings positioned at 16.67%C, 25.0%C, 33.33%C, 41.67%C, and 50.0%C. The longest PO afterbody has its focus at the 16.67% chord point. As will become evident shortly, one wants to place the focus as far forward on the shroud as possible, yet at the same time minimize the PO weight penalty. For the LTD machine, this compromise was reached by placing the focus at 33.33%C. Note that the PO contours in Fig. 4 bear a striking resemblance to isentropic spike rocket engine nozzles.

Graham and Bergman were the first to build plug nozzle rocket engines back in the late 50's and early 60's while working for General Electric.[9] Figure 5 shows their 16,000 lb (71.2 kN) thrust, H_2O_2 uncooled plug nozzle thrust chamber mounted in a test cell. Incidentally, this engine developed a thrust level roughly equivalent to the LTD engine's maximum thrust in the airbreathing mode. As indicated in Fig. 6, six H_2O_2 decomposers were arranged around the base of the plug to provide exhaust gases for hot tests. Two, of the many external expansion nozzles which were tested, are displayed in Figs. 6A and 6B; an isentropic plug, and a 20° foreshortened plug. This rocket engine demonstrated good performance at off-design pressure ratios, and proved the feasibility of thrust vector control by selective combustor throttling. Subsequent analysis of the test data revealed that full isentropic plug nozzles could be subjected to substantial truncation/foreshortening, without degrading the thrust performance to any large degree. Figure 7 indicates the method used to foreshorten the plug nozzles, by replacing the tip with a cone at the appropriate tangent location.

For the first flight-weight demonstration of a regeneratively cooled plug nozzle rocket engine, Graham and Bergman decided to completely truncate the isentropic spike nozzle, replacing it altogether with the 42° half-angle cone shown in Fig. 8. Calculations were carried out to determine the minimum size of plug nozzle that could cool

COMPONENT	MASS (Kg)	
LN_2 PROPELLANT TANK	33.4	
REGEN.-COOLED PRIMARY OPTIC	33.0	
SHROUD & INJECTOR PLATES	15.0	
ELECTRONICS & C³I	18.0	
TPS TILE (&C-C NOSE)	5.0	
ATTITUDE CONTROL SYSTEM	2.7	
HIGH PRESSURE H_E TANK (INCL. REGULATOR)	3.2	
INTERCONNECTING STRUCTURE	8.6	
DRY MASS	120.0 Kg	PAYLOAD
ULLAGE (LN_2)	30.0 Kg	PAYLOAD
LN_2 PROPELLANT	150.0 Kg	
TOTAL LAUNCH MASS	300.0 Kg	

Table 2: LTD Mass Breakdown

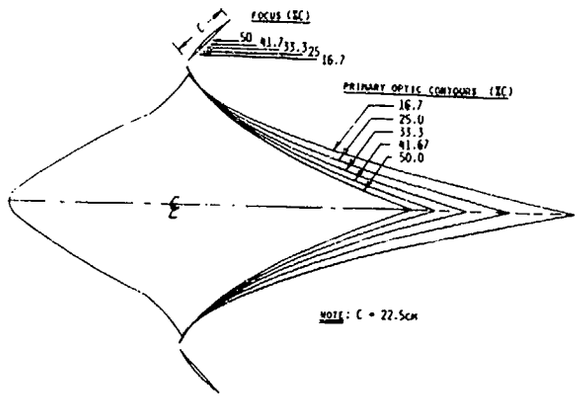

Figure 4: Primary Optic Contours vs. Focal Locations

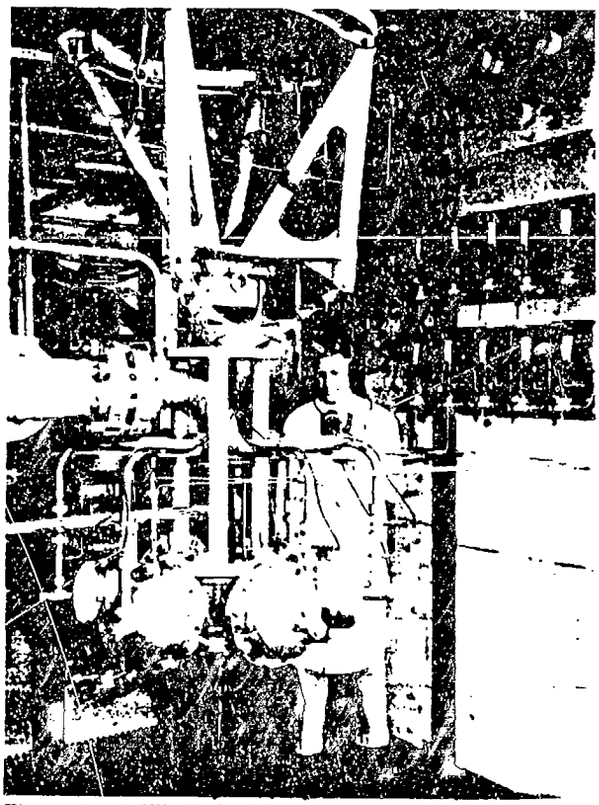

Figure 5: 16 Klb H_2O_2 Plug Nozzle Development Thrust Chamber in Test Cell (After Graham and Bergman, Ref. [9])

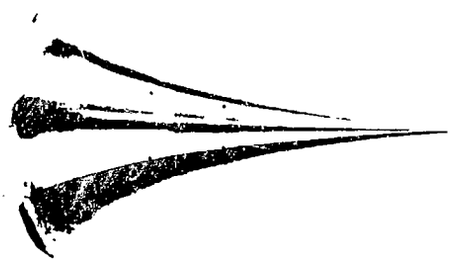

Figure 7: Isentropic Plug Nozzle, External Expansion (from Ref. [9])

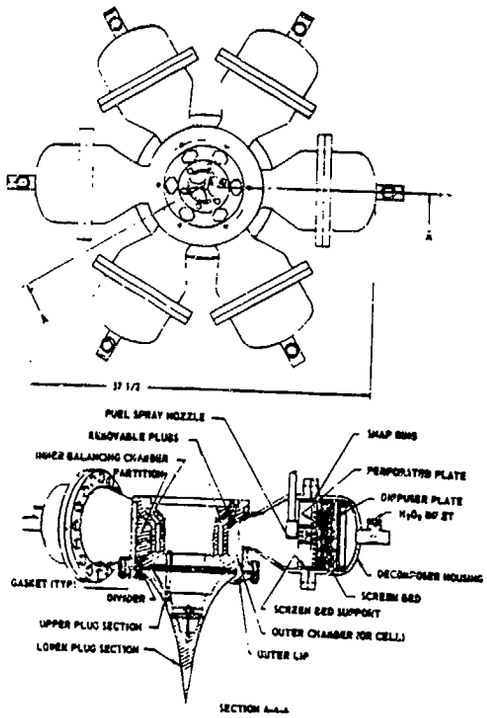

Figure 6: Detail of 16 Klb H_2O_2 Plug Nozzle Configuration (from Ref. [9])

itself with RP-1/LOX propellants. The result was the 50,000 lb thrust stainless steel engine displayed in Fig. 9. As indicated in Fig. 10, the plug nozzle had an exit nozzle diameter of 1.07 m (which is identical to that of the primary optic of the LTD machine). The overall maximum diameter of the 50,000 lb thrust engine was 1.34 m.

Figure 11 shows one of the eight cooled segments of which the engine is composed; each segment could be independently throttled to accomplish thrust vectoring. Pictured in Fig. 12 is an enlarged view of the lower cone segment, revealing the RP-1 coolant flow passageways.

The lower cone segments were fabricated from two thin stainless steel faceplates separated by numerous vertical ribs that formed the coolant passageways, all fused together by an electron-beam welding machine. Each of the eight lower cone segments had a mass of 2.077 kg and an area of 1089 cm^2; this translates to a mass penalty of 1.9 grams for every 1 cm^2 of regeneratively cooled surface area.

It is interesting to imagine how this method of construction might be applied to the design of a cooled primary optic for the LTD spacecraft. Similar techniques are no doubt being investigated for large cooled optics in SDI power-beaming applications. The shortest primary optic contour in Fig. 4 (i.e., focus at 50%C) has a total surface area of 17370 cm^2. At 1.9 g/cm^2, a stainless steel mirror might come in at 33 kg. Using aluminum, perhaps the 33.3%C optic could be built for the same total mass. A schematic diagram showing the internal details of this primary optic design is given in Fig. 13.

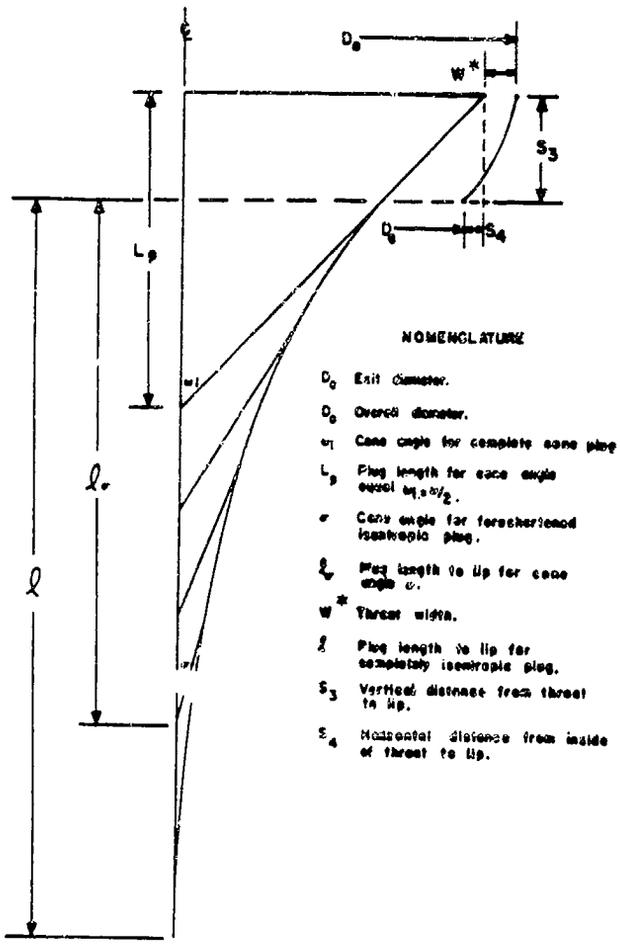

Figure 8: Outline of 50 Percent Internal Expansion Plug Nozzle (from Ref. [9])

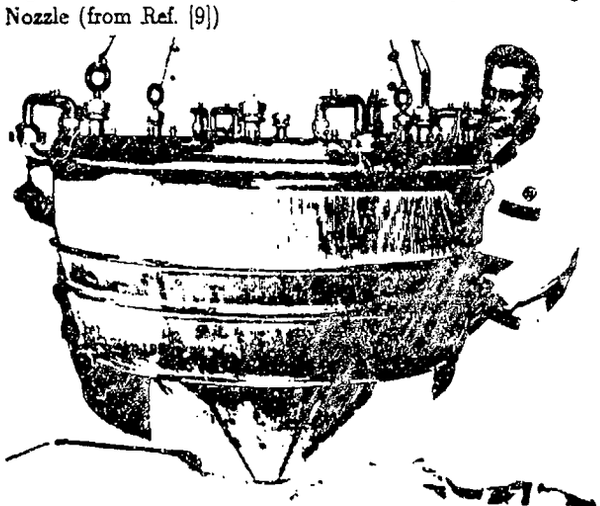

Figure 9: Cooled Engine Prior to Wire Wrapping and Thrust Mount Installation (from Ref. [9])

Injector Head

Pictured in Fig. 14 is one of the eight ring injectors that forms a complete annulus at the top of the 50 Klb thrust rocket engine. One might envision a similar injector head, reduced in width to 1 cm, for the LTD spacecraft

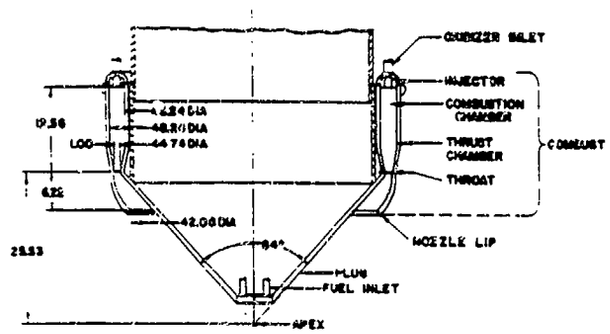

Figure 10: 50 Klb Plug Nozzle Configuration (Dimensions in inches) (from Ref. [9])

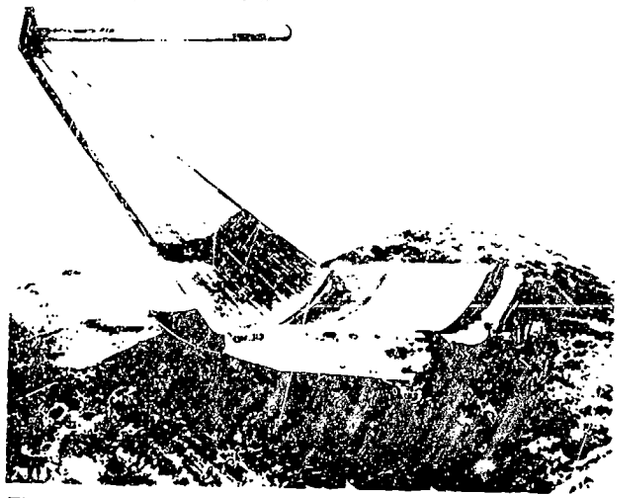

Figure 11: Cooled Segment, (from Ref. [9])

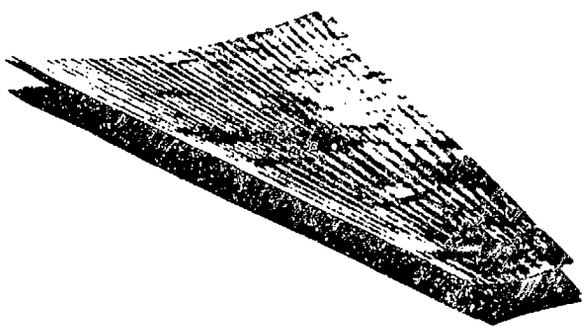

Figure 12: Cone Segment Assembly (from Ref. [9])

at the engine's annular focus region. As will be discussed below, laser supported detonation (LSD) waves must be ignited at this location with absolute rehability. Therefore, these injector heads could perhaps be covered with a tuned ignition array[10,11] or other material to minimize the beam energy and time required to ignite LSD waves. Other "hot section" surface areas which must be actively cooled within the LTD engine (see Fig. 3) include the shroud support struts, leading edge of the shroud airfoil, and entire lower flat surface of the airfoil — which is the primary impulse coupling region.

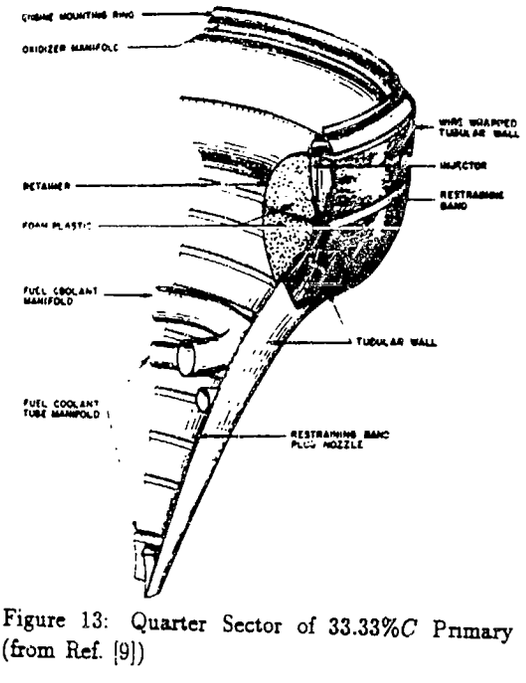

Figure 13: Quarter Sector of 33.33%C Primary Optic (from Ref. [9])

Mechanical Layout of the LTD Spacecraft

Now that the most massive LTD spacecraft items (such as the 70 cm diameter LN_2 propellant tank, regeneratively cooled primary optic, and rocket propellant injector head) have been described, the general spacecraft mechanical layout can be presented. With regard to the LTD cutaway view shown in Fig. 3, note that the entire external compression inlet forebody of the LTD is covered with black Thermal Protection System (TPS) tile, similar to that used on the shuttle orbiter lower heat-shield surface. Due to the high stagnation conditions at the LTD's nose, this region must also be capped with the same carbon/carbon material used on the Shuttle nose and wing leading edges. On the LTD, this lightweight thermal protection system will be fastened to a carbon/epoxy composite substructure that attaches directly to the LN_2 tank. The spherical, filament-wound Kevlar LN_2 tank serves as a structural backbone for the entire LTD vehicle, to which all subcomponents are rigidly attached.

Note in Fig. 3, that the electronics/instrumentation compartment resides in the nose section just forward of the LN_2 tank. Also located in this region are the cold N_2 gas jets required for spacecraft attitude control in the satellite mode. For spin-stabilization, additional jets would be placed out near the shroud, but still in the centerbody volume.

As well stated by Fuhs and Masier,[3] "Sounding rockets, rather than scaled down satellites, are the best model for lightsat design, fabrication and operation." The LTD spacecraft can certainly be categorized as a lightsat, where cost is of prime concern. For this reason, the cost and increased complexity of the H_2O_2 attitude control systems are abandoned in favor of simpler cold gas jets. A small solar array could be integrated with the upper surface of the

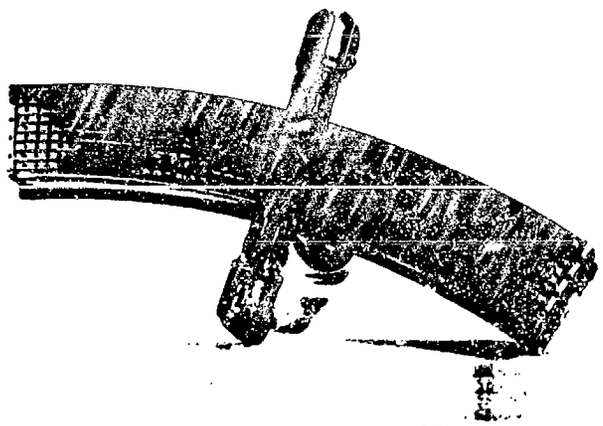

Figure 14: Injector Model III (from Ref. [9])

shroud and would recharge a few batteries when bathed in sunlight. Simple discrete devices would be used for power conditioning and regulation.

Finally, the advanced microelectronics used for signal processing, data transmission, guidance and control must be powerful enough to carry out multiple missions: (1) laser boost phase, and (2) satellite phase.

As indicated in Fig. 3, the annular shroud is firmly affixed to the LN_2 tank by way of a special shock-damping mechanism that attempts to isolate the primary optics and the rest of the spacecraft from the vibrating shroud element. Most of the thrust developed by the repetitively-pulsed combined-cycle engine is communicated directly to the shroud. Perhaps computer controlled active damping structures technology can be applied here.

A few comments should be made about the shroud's mechanical construction. As noted in Fig. 3, the shroud may have a trailing edge flap to act as a variable area nozzle, and also, perhaps to reduce the vehicle's frontal area (and hence, drag) when in an unpowered "coasting" mode within the atmosphere. The shroud structure will probably be the most abused of any in the spacecraft, and must be exceedingly strong. Perhaps this is the place for high temperature metal matrix composites and refractory materials.

When transitioning between airbreathing and rocket modes, servo-mechanical actuators will deploy shutters to close off the annular air gap (i.e., between the LTD centerbody and shroud) to shut off the air flow. At this time the propulsion mode becomes a pure rocket, and the LN_2 mass flow rate is increased dramatically by the pressure regulator. In this regard, it is appropriate to describe the propellant management system. Because of the small size of the LN_2 tank, the most expedient and reliable propellant delivery system would be to simply pressurize the tank. This approach is not accessible to less efficient propulsive systems which require a very large volume of propellants because tank weight quickly becomes prohibitive. Hence, a separate, small (25-30 cm diameter), high pressure (e.g., 5 to 6 Kpsi) tank (perhaps carbon fiber wound) and regulator is invoked for the LTD propellant delivery system.

Optical Systems Layout

For the LTD spacecraft, the primary optic can be designed to operate in four basic roles: (1) primary concentrating optic for laser propulsion, (2) sensor, (3) transmitter aperture, (4) receiver aperture. To make the transition between the first and second roles, an advanced sensor array (i.e., retina) would be deployed, by servo-mechanical actuators, into the 1 cm wide focal region of the PO mirror. Then, data from this distributed "insect eye" retina would be combined electronically or optically (like the six eye multiple mirror telescope) into a single high quality image.

To transition into the receive/transmit role, perhaps low power monolithic microwave integrated circuits (MMIC) can be used to drive phased-array elements (positioned in the focal region of the parabolic PO). As suggested by Browde in Ref. [3], this should be a good way to cut the weight of the radio frequency radiator and receive/transmit electronics, while providing an electronic means of beam steering.

Description of Airbreathing Propulsion Mode

The LTD machine will utilize a combined-cycle engine design. The design incorporates both airbreathing and rocket modes of operation. The airbreathing mode is a form of External Radiation-Heated (ERH) thruster.[6,7] In this engine concept, a laser induced plasma is ignited on the lower surface of the shroud. This high pressure (e.g., 600 atm) plasma bubble expands as it is convected down the surface of the shroud. The expansion yields a higher pressure on the aft side of the shroud, producing a forward thrust. This "shroud lift" ERH thruster is pictured in Fig. 15. The performance of this engine is demonstrated in Figures 16, 17, and 18. The reader is encouraged to examine Ref. [7] for a detailed description of this propulsion concept.

Analysis of LTD Vehicle Inlet Flow

In order to analyze the performance of the airbreathing engine, it was necessary to model the LTD vehicle's inlet flowfield. The basic assumptions that had to be made were mainly for the simplification of the analysis. While it was important that an accurate model of the flow over the vehicle forebody be developed, a simplified model had to be developed first. In the construction of the model, it was held in perspective that the optimization of the flow of fresh air to the thrust area was to be the primary objective. This flow of fresh air was necessary to solve the "refresh" problem that occurs with such a pulsed engine.

Assumptions Made in the Analysis

It was of great importance that the air velocity at the location of thrust generation be as high as possible. This could best be achieved by using a vehicle forebody that was as slender as possible for supersonic flow and yet still satisfactory for subsonic flow. It was assumed that the flow was largely inviscid, although some viscous effects would eventually be included during the evolution of the model. The flow is dominated by compressible flow effects since the flight regime of interest could go up to Mach 8. The forebody was modeled as a double cone, made up of 30°, and a 45°, semi-vertex angle cones.

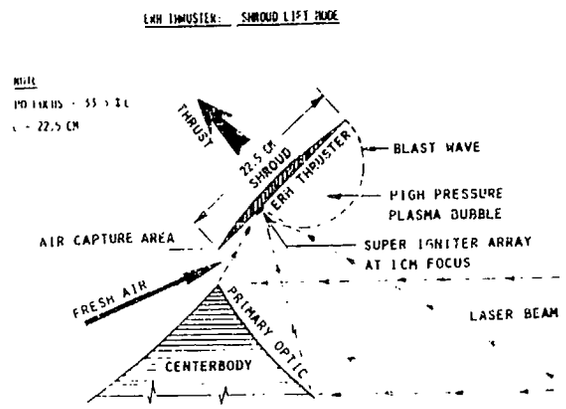

Figure 15: ERH Thruster: Shroud Lift Mode

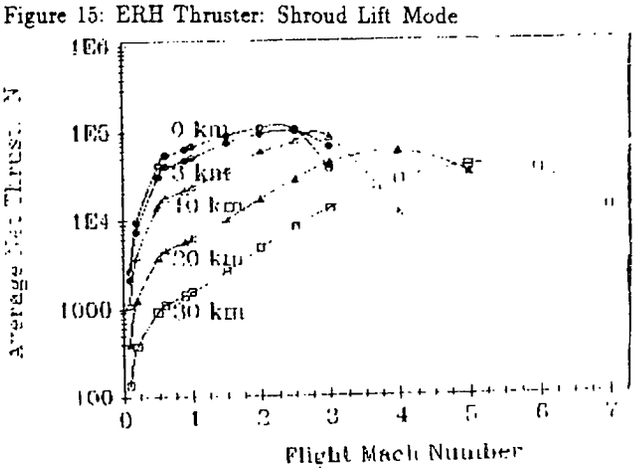

Figure 16: "Shroud Lift" ERH Thruster: Average Net Thrust

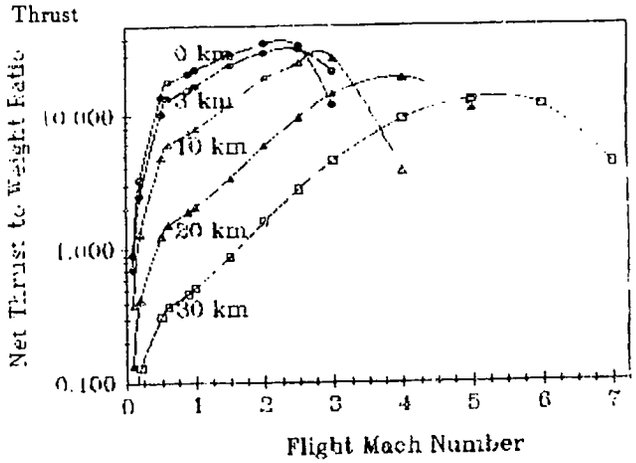

Figure 17: "Shroud Lift" ERH Thruster: Net Thrust to Weight Ratio

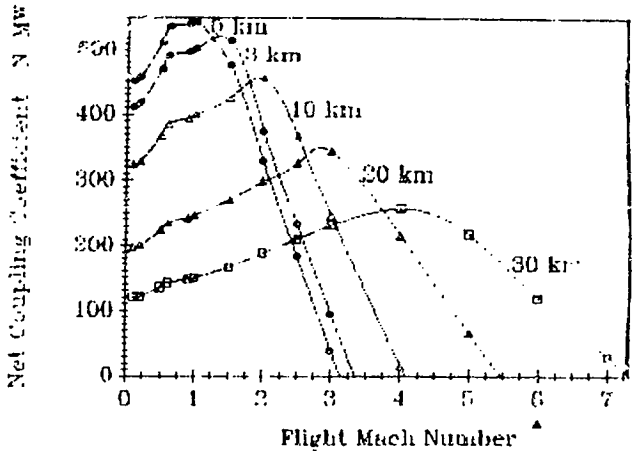

Figure 18: "Shroud Lift" ERH Thruster: Coupling Coefficient

To determine the velocity at the flow location, it was necessary to know the velocity of the air at the entrance of the shroud region. The latter required knowledge of the velocity over each of the cones making up the vehicle forebody.

For the subsonic part of the flight regime, it was assumed that the ratio of the maximum air velocity over the cone to the freestream velocity was similar to that over cones and/or spheres. For this vehicle, a ratio of inlet to freestream Mach number of 5 to 3 was assumed until the inlet velocity reached sonic value, and then it was assumed to remain approximately equal to one ($M_{in} = 1$) for the subsonic part of the flight.

Analytical Procedure

With the inlet Mach number schedule assumed above, one less parameter was needed for the determination of the inlet velocity and mass flow rate. These values are needed for the calculation of the thrust-area refresh air velocity and the vehicle ram drag.

For supersonic flow conditions, the shocks formed over the vehicle forebody rendered the analysis a bit tedious. The Mach number after the oblique shock over the first cone forming the vehicle forebody was calculated with the oblique shock relations for a wedge. The same type of relations were used to calculate the stagnation pressure ratio p_{t_1}/p_{t_a}, and static pressure ratio, p_1/p_a across the shock as well as the shock angle.

Once the Mach number after the first oblique shock (M_1) was known, the same process was employed in calculating the Mach number after the shock over the second cone (M_2), the pressure ratios p_{t_2}/p_{t_a} and p_2/p_a, and the shock angle, if M_1 was supersonic.

The overall pressure recovery of the vehicle inlet is the stagnation pressure ratio from the inlet to freestream. This is obtained by multiplying the stagnation pressure ratios after the first and second shocks. Note that the inlet itself would have a normal shock which may reduce the refresh air Mach number to below the inlet Mach number schedule assumed. This and other assumptions are to be verified by more detailed models later.

With the above information, the inlet velocity can now be calculated as:

$$u_{in} = \sqrt{\frac{\gamma p_{in}}{\rho_{in}}} \tag{4}$$

where p_{in}, the inlet pressure, and ρ_{in}, the air density at the inlet, can be calculated from the ambient pressure, p_a, and the freestream Mach number, M_a, with

$$\frac{p_{in}}{p_a} = \left(\frac{1 - \frac{(\gamma-1)}{2} M_a^2}{1 - \frac{(\gamma-1)}{2} M_{in}^2} \right)^{\frac{\gamma}{(\gamma-1)}} \frac{p_{t_2}}{p_{t_1}} \frac{p_{t_1}}{p_{t_a}} \tag{5}$$

$$\frac{\rho_{in}}{\rho_a} = \left(\frac{p_{in}}{p_a} \right)^{\frac{1}{\gamma}} \tag{6}$$

The ram drag can be calculated as:

$$D_{RAM} = \dot{m} u_{in} \tag{7}$$

where

$$\dot{m} = \rho_{in} u_{in} A_{inlet} \tag{8}$$

The pressure recovery schedule, determined from the above calculations, is presented in Fig. 19.

Trajectory Simulation

The trajectory simulation of the LTD was done on McDonald Douglas' Simulation and Optimization of Rocket Trajectories (SORT)[12] computer program. Three different launch angle cases of 30°, 45° and 60° (measured from horizontal) were run on the program.

In each case the LTD machine was given an initial velocity of 100 m/sec. At 0.5 sec the shroud lift ERH thrusters were engaged and the vehicle was flown until it reached a Mach number of 7.0, the upper limit of ERH thruster performance. When this velocity is attained, the ERH thruster model switches to the scramjet model and flies to an altitude of 160 kft. At this point the engines shut off and the LTD vehicle cruises until it reaches the highest altitude before diving back to earth. The craft is then pitched over to 0° with respect to the horizon and the laser heated rockets are engaged, accelerating the LTD to orbital velocity of 8 km/sec.

Figures 20 to 25 show the results of running the SORT program. The 30° initial angle case is the most undesirable of the three cases flown. In this case the vehicle starts to return to earth instead of entering orbit. The LTD also uses more power then is allowed (250 MW) for this vehicle. The 60° case obtains orbital velocity sooner and a greater altitude but uses too much fuel in the rocket mode in reaching orbital velocity.

In all three cases the scramjet only operates for a few seconds and does not add much acceleration to the LTD machine. This is due to the fact that the craft climbs through the atmosphere very quickly and attains altitudes where the scramjet produces very little thrust.

To compare a different mission profile, an LTD trajectory was run at 30° initial launch angle with the craft switching from shroud lift ERH thruster directly to laser-heated rocket. This mission bypasses the scramjet mode,

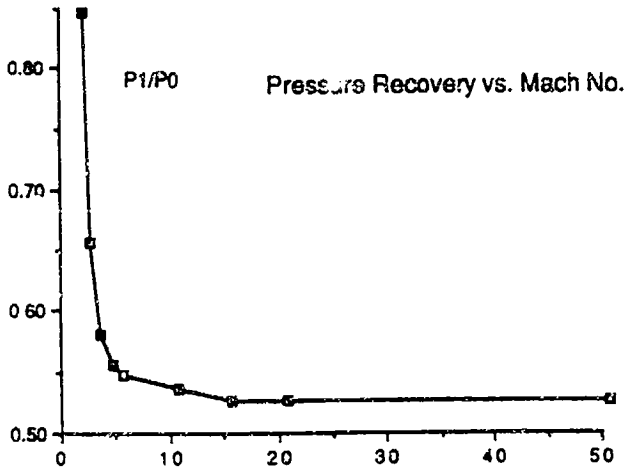

Figure 19: Pressure Recovery (p_i/p_a) vs. Flight Mach Number for the LTD Inlet

which the first three cases use. The specific impulse (I_{sp}) for the rocket was raised from 650 seconds to 875 seconds. Figures 26 to 31 show the performance of the LTD machine for this run. The craft climbs more quickly and travels further downrange than the first three cases while having a longer rocket phase. The greater specific impulse allows the craft to have a larger final mass as it goes into orbit.

The first three cases are useful for Low Earth Orbit missions while the ERH/Rocket mode can be used for higher altitude operations. In both these cases an onboard chemical rocket or a laser relay satellite is needed for the final thrust into orbital insertion.

Conclusions

The proposed Lightcraft Technology Demonstrator should create a significant economic impact. Since the LTD machine integrates a laser propulsion engine with the satellite hardware it results in a decrease in both launch costs and payload costs. The single-stage-to-orbit spacecraft becomes a sensor satellite after arrival in orbit. The LTD's dry mass of 120 kg plus 30 kg of LN_2 ullage represents the entire payload. This payload, containing the 1 meter diameter optic, is suitable for a sensor satellite mission at altitudes up to 2000 km. Since the laser propulsion engine and satellite functional hardware are shared, the LTD concept can lower both *launch* and satellite *payload* costs by an order of magnitude, or more.

The LTD machine utilizes a combined-cycle engine to reach orbit. This approach was chosen over an all-rocket system because of the need to reduce liftoff mass. The airbreathing boost to Mach 7 and 30 km altitude enables a vehicle mass ratio of 2.0 to LEO. An all-rocket approach would require a liftoff mass of 1000 kg to put the same 150 kg into orbit. The combined-cycle engine can do the same mission with a liftoff mass of 300 kg. Since airbreathing engines have impulse coupling coefficients (CC) of 2× to 4× greater than rockets, laser-boosted spacecraft with combined-cycle engines will outperform those with only rocket engines.

Liquid nitrogen was chosen as the propellant/coolant for the LTD machine. Although liquid hydrogen would give the highest specific impulse, its low density would allow only 14 kg to fit in the proposed 70 cm diameter tank. Water has been examined as a possible fuel for laser-energized engines, but was found to be inappropriate in this case. Water would result in an exhaust plume that is highly absorbent to the suggested 10.6 μm radiation. Liquid N_2 has a density only a little less than that of H_2O (80.8%), allowing 180 kg to fit in the propellant tank. Also, N_2 has properties close to those of air, which is 78% N_2 by volume. This will simplify the transition between airbreathing and rocket modes. Additionally, LN_2 is inert, and will not contaminate the high power laser optics, and LN_2 cooled aluminum mirrors have been developed for SDI. A nitrogen fueled laser-heated rocket would have a specific impulse (I_{sp}) of 725 to 1025 sec.

Finally, it should be emphasized that the technology for the LTD machine exists today. Several critical "proof-of-concept" experiments for pulsed laser propulsion have already been demonstrated. The required ground based laser (GBL) system could be constructed with materials and technology that has been in existence for 15 years. The optics, fuel management system, and plug nozzle are all possible with present technology. Although certain aspects of the design could be improved with advanced technology, the proposed concept is a near-term, realistic demonstration of the feasibility and usefulness of laser-energized propulsion.

References

[1] Canavan, G. H., "Laser Propulsion of Sensors and Interceptors," LA-UR-87-3208, Los Alamos National Laboratory, Los Alamos, NM, 1987.

[2] Canavan, G. H., "Decoy Deployment with Laser Propulsion," LA-UR-88-1246, Los Alamos National Laboratory, Los Alamos, NM, April 1988.

[3] Fuhs, A. E. and Mosier, M. R., "A Niche for Lightweight Satellites," *Aerospace America*, April 1988, pp 14–26 and 36.

[4] Mozey, R., "The Cost of Lifting Weapons to Space," Center for International Security and Arms Control, Stanford University, Stanford, CA, Oct. 1986.

[5] "Proceedings of the First SDIO/DARPA Workshop on Laser Propulsion," J. T. Kare, Technical Editor, Lawrence Livermore National Laboratory, CONF-860778, Livermore, CA, 7–18 July 1986.

[6] Myrabo, L. N., editor,"The Apollo Lightcraft Project," NASA/USRA Advanced Design Program, 3rd Annual Summer Conference, Washington, D.C., 17–19 June 1987.

[7] Smith, W. L., editor, "The Apollo Lightcraft Project," Vol. 2. NASA/USRA Advanced Design Program, 4th Annual Summer Conference, Kennedy Space Center, Florida, 13–17 June 1988.

[8] Personal Communication, Spawr, W. and Pierce, R., SPAWR Optical Research, Corona, CA, 1988.

[9] Graham, A. R., "NASA Plug Nozzle Handbook," Contract NAS9-3748, General Electric Co., for the New York State Atomic and Space Development Authority, circa 1970.

[10] Reilly, D. A., "Advanced Propellant for Laser Propulsion," presented to the 1987 SDIO Workshop on Laser Propulsion, Los Alamos National Laboratory, Los Alamos, NM, 14–18 Sept. 1987.

[11] Rollins, C., and Weyl, G., "Issues for Laser Propulsion: Progress in Theory and Modeling," presented to the 1987 SDIO Workshop on Laser Propulsion, Los Alamos National Laboratory, Los Alamos, NM, 14–18 Sept. 1987.

[12] Berning, M., "Version IV User's Guide for the Simulation and Optimization of Rocket Trajectories Program," McDonnell Douglas Astronautics Co., Houston, TX, Transmittal Memo No. 1.2-TM-FM86028-53, Dec. 1985.

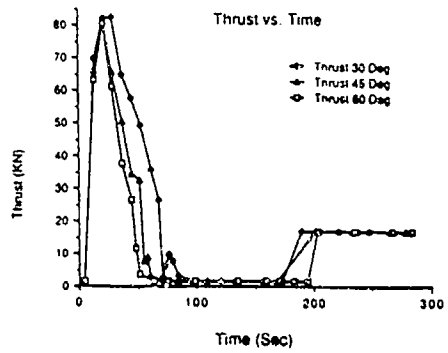

Figure 20: Thrust vs. Time

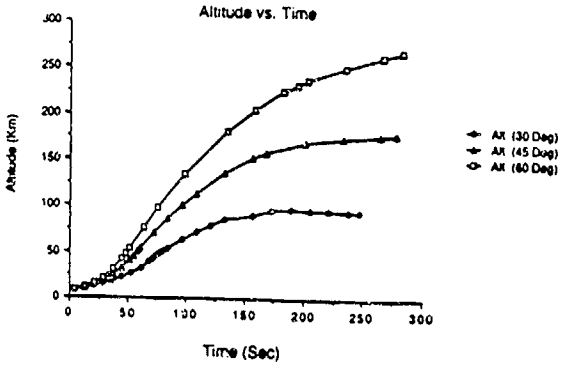

Figure 21: Altitude vs. Time

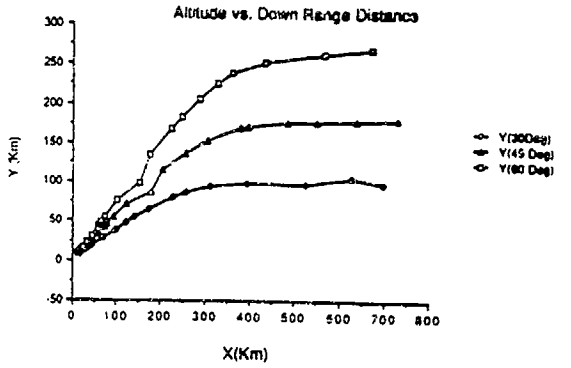

Figure 22: Trajectory (Altitude vs. Downrange Distance)

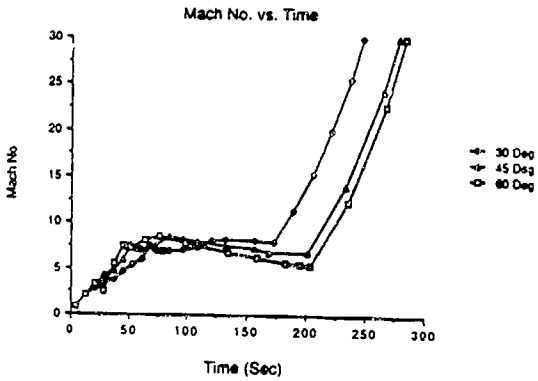

Figure 23: Flight Mach Number vs. Time

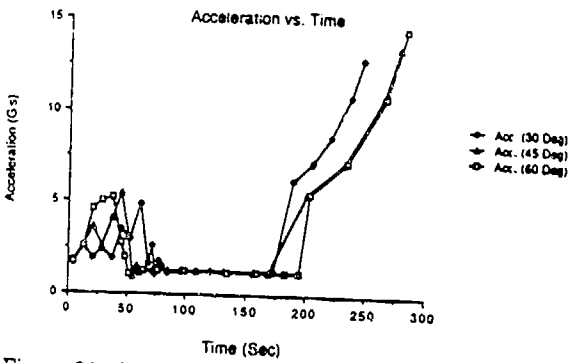

Figure 24: Acceleration vs. Time

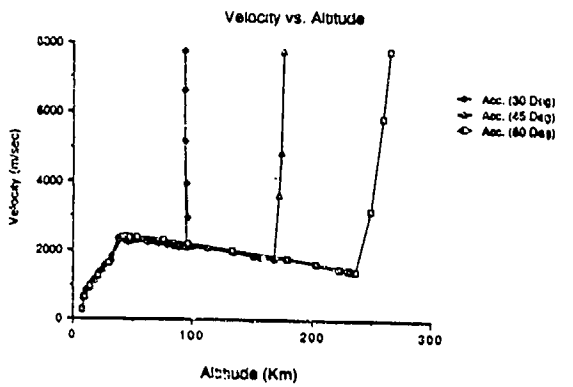

Figure 25: Velocity vs. Altitude

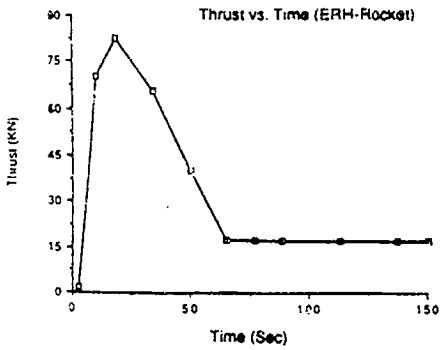

Figure 26: Thrust vs. Time (ERH-Rocket Only)

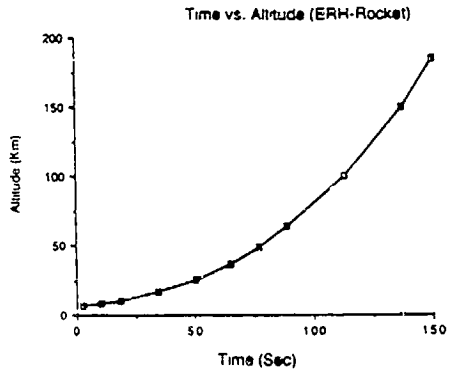

Figure 27: Altitude vs. Time (ERH-Rocket Only)

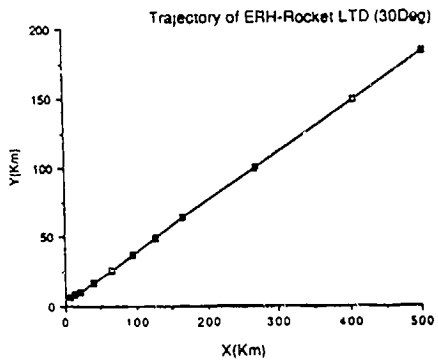

Figure 28: Trajectory (Altitude vs. Downrange Distance) (ERH-Rocket Only)

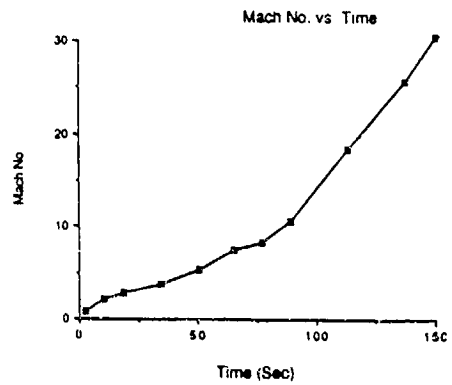

Figure 29: Flight Mach Number vs. Time (ERH-Rocket Only)

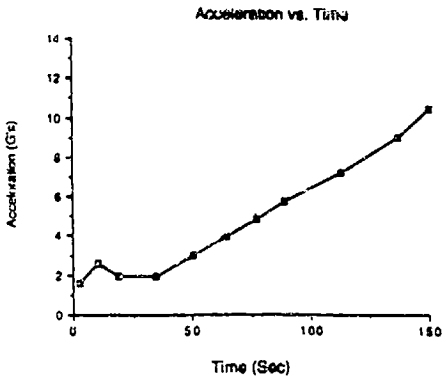

Figure 30: Acceleration vs. Time (ERH-Rocket Only)

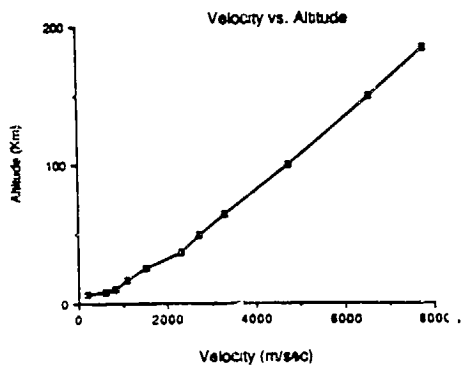

Figure 31: Velocity vs. Altitude (ERH-Rocket Only)